Research Article Adv. Mater. Lett. 2015, **6**(9), 834-839 Advanced Materials Letters

www.amlett.com, www.vbripress.com/aml, DOI: 10.5185/amlett.2015.5920 Published online by the VBRI Press in 2015

Structural, electrical and optical properties of molybdenum doped zinc oxide films formed by magnetron sputtering

R. Subba Reddy[1*], K. Radhamma[1], A. Sivasankar Reddy [2], S. Uthanna[1]

[1]*Department of Physics, Sri Venkateswara University, Tirupati 517502, India*
[2]*Department of Physics, Vikrama Simhapuri University, Kavali 524201, India*

[*]Corresponding author. E-mail: sbbreddy82@gmail.com

Received: 28 February 2015, Revised: 21 April 2015 and Accepted: 06 May 2015

ABSTRACT

Thin films of molybdenum doped (2.7 at.%) zinc oxide (MZO) were deposited on glass substrates held at room temperature by RF magnetron sputtering of mosaic target of Mo-Zn at different substrate bias voltages. The influence of substrate bias voltage on the structural, electrical and optical properties was investigated. The MZO films deposited on unbiased substrate were of amorphous, while those formed at substrate bias voltage of -40 V and above were of nanocrystalline. The crystallite size of the films improved with the applied bias voltage. At higher substrate bias voltage of -120 V the ion bombardment induced the high defect density in the films hence decrease in the crystallinity. The films formed at substrate bias voltage of -80 V exhibited low electrical resistivity of 1.2×10^{-2} Ωcm and optical transmittance of about 79 %. These films showed optical band gap of 3.29 eV and figure of merit of 19 $\Omega^{-1}cm^{-1}$.

Keywords: Thin films; Mo-ZnO films; sputtering; structure; optical properties.

Introduction

Zinc oxide is wide band gap (3.37 eV) semiconductor with large exciton binding energy (60 meV) which allow efficient lasing mechanism at room temperature. It is nontoxic, inexpensive, abundant and mechanically stable. In find potential applications as transparent conducting oxides, photovoltaic cells, gas sensors, light emitting diodes and photocatalyst in water treatment [**1-4**]. Thin films of pure ZnO formed by various thin film deposition techniques were of low electrical conductivity. In order to enhance the electrical conductivity, doping of suitable metals with ZnO is essential for its application in transparent conductors in thin film solar cells and in transparent thin film transistors. One of the methods improving the electrical conductivity is by doping of ZnO with aluminium[**5-8**], gallium [**9, 10**], boron [**4**], tungsten [**11**], tin [**1**], copper [**12**], phosphorous [**13**] or molybdenum [**14**] etc. Doping of molybdenum in ZnO films (MZO) is interesting since it contributes more than one carrier for the electrical transport hence increase in the electrical conductivity while keeping high optical transmittance in the visible region. Moreover its ionic radius (0.046 nm and 0.041 nm for Mo^{5+} and Mo^{6+}) is close to Zn^{2+} (0.060 nm) when compared to Al^{3+} (0.039 nm) therefore molybdenum substitution of zinc ions of the host matrix than interstitial positions [**15**]. Thin films of MZO have been formed by RF /DC magnetron sputtering [**15-18**], co-sputtering [**19**], ion beam deposition [**20**] and spray pyrolysis [**21**]. In the present work, an attempt is made in the deposition of Mo doped ZnO thin films by reactive RF magnetron sputtering at different substrate bias voltages in the range from 0 to -120 V. The deposited films were characterized for their structural, surface morphological, electrical and optical properties and studied the influence of substrate bias voltage on the physical properties.

Experimental

Thin films of MZO were deposited on glass substrates using RF magnetron sputtering technique. The sputter chamber was evacuated to the base pressure of 5×10^{-4} Pa using rotary pump - diffusion combination. Pure Zn target of 50 mm diameter and 3 mm thick covered with molybdenum strips in the sputtered zone was used for preparation of the experimental films. Films were deposited in the sputter down configuration. The MZO films were formed on glass substrates held at room temperature and at oxygen partial pressure of 2×10^{-1}Pa, sputter pressure of 5 Pa and at different substrate bias voltages (V_b) in the range from 0 to -120 V. Thick aluminum film on the bottom of the glass substrate was deposited by thermal evaporation in order to apply bias voltage to the substrate. Unbalanced magnetron was used for the deposition of the films. The RF power (Advanced Energy Model ATX-600 W) fed to the sputter target was 50 W. Sputter parameters maintained for the deposition of MZO films were given in the **Table 1.**The deposited MZO films characterized for their chemical composition, structure and surface morphology, electrical and optical properties.

Table 1. Deposition parameters fixed for the growth of molybdenum doped zinc oxide (MZO) films.

Sputter target	Zn target (covered with Mo strips)
Target to substrate distance	50 mm
Base pressure	$5x10^{-4}$ Pa
Oxygen partial pressure (pO_2)	$2x10^{-1}$ Pa
Sputter pressure	5 Pa
Sputter power	50 W
Substrate bias voltage (V_b)	0 to -120 V
Film deposition time	60 min.

The thickness of deposited films was measured with α-step profilometer (Veeco Dektak Model 150). Diamond stylus with cone angle of 45^o (60^o) with tip diameter of 0.5 micrometer was employed to scan the surface of the film. Chemical composition of the deposited films was determined with energy dispersive X-ray analyser (EDAX Oxford Instruments Inca Penta FETX3) attached to the scanning electron microscope (Carl Zeiss Model EVO MA 15) to an accuracy of about 0.5 at.%. The crystallographic structure of the films was determined with Bruker D8 Advanced Diffractometer at the glancing angle of 4^o with Cobalt X-ray radiation with wavelength of 0.17889 nm and scanned with step of 0.02^o per minute. Surface morphology was analyzed by atomic force microscope (Bench Apparatus Digital Instruments Model 3100) in non-contact mode. The electrical resistivity of the films was determined using standard four point probe method. The optical transmittance of the films was recorded in the wavelength range 300-1200 nm using Hitachi (Model U 3400) double beam spectrophotometer with accuracy in the wavelength of 0.5 nm.

Results and discussion

The thickness of the deposited MZO films measured by depth profilometer was in the range 190 - 220 nm. Deposition rate of the films was calculated from the thickness (t) and the duration of deposition. The deposition rate of the films increased from 3.2 to 3.7 nm/min with increase of substrate bias voltage from 0 V to -80 V, there after decreased to 3.4 nm/min at higher substrate bias voltage of -120 V. The increase of deposition rate with increase of bias voltage at low voltage range was due to attracting the positively charged molecules and clusters of the sputtered material in the plasma, which incorporate the sputtered material to arrive on the surface of the substrate. Yang et al. [**22**] noticed such dependence of deposition rate on the bias voltage in RF sputter deposited indium tin oxide thin films. Chemical composition of the MZO films was determined by using energy dispersive X-ray analysis (EDAX) from the intensity of the characteristic peaks of molybdenum, zinc and oxygen. **Fig. 1** showed the EDAX spectrum of Mo-ZnO film formed on unbiased substrate. Chemical composition of the deposited film was Zn = 47.5 at. %, O = 49.8 at. % and Mo = 2.7 at. % which indicated that molybdenum substituted the zinc in the ZnO films. It remained almost constant in all the films formed at different substrate bias voltages.

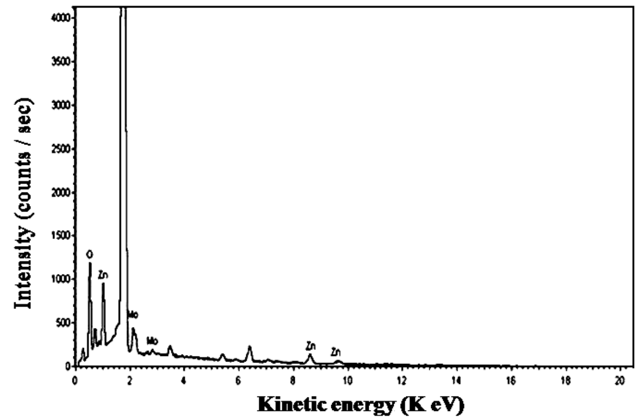

Fig. 1. EDAX spectrum of MZO films formed on unbiased substrate.

Fig. 2 shows the X-ray diffraction profiles of MZO films formed at different substrate bias voltages. The MZO films formed under unbiased substrates does not contain any diffraction reflections revealed that the grown films were in amorphous nature.

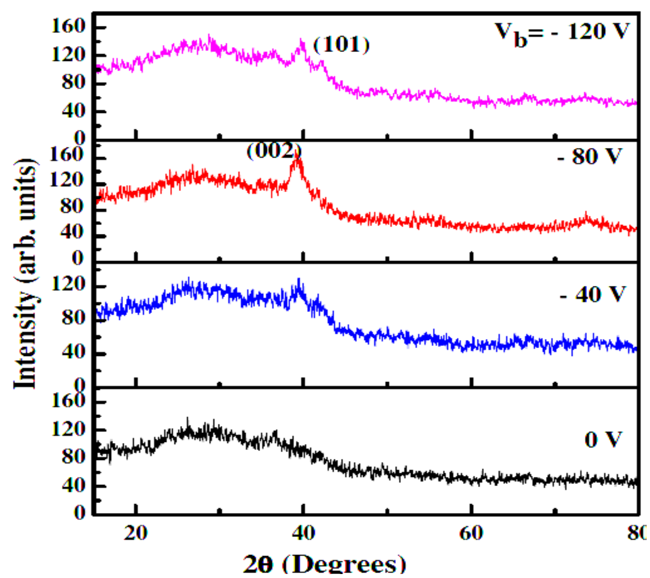

Fig. 2. X-ray diffraction profiles of MZO films formed at different substrate bias voltages.

The films formed at substrate bias voltage of -40 V exhibited a broad diffraction peak of (002) reflection of zinc oxide films with wurtzite structure. Further increase of substrate bias voltage to -80 V, the intensity of diffraction peak enhanced due to improvement in the crystallinity of the films. At higher substrate bias voltages that is -120 V, the intensity of the (002) reflection reduced with presence of an additional weak (101) reflection. At higher substrate bias voltages, the ion bombardments induces high defect density in the films and re-sputter hence decrease in the crystallinity [**23**]. Such an enhancement in the crystallinity with the increase of substrate bias voltage was noticed in sputtered TiO_2 films [**24**] and in pure ZnO films [**25**]. The crystalline size (L) of the films was calculated from the X-ray diffraction peak using the Debye - Scherrer's relation,

$$L = k\,\lambda / \beta \cos\theta \qquad (1)$$

where, k is a constant and β the full width at half maximum intensity. The crystallite size of the films increased from 5.2 to 9.8 nm with increase of substrate bias voltage from -40 to -80 V, there after decreased to 7.5 nm at higher substrate bias voltage of -120 V. **Fig. 3** shows the AFM two- and three dimensional images of MZO films formed at different substrate bias voltages. The grains were uniform in the size and the size of the grains influenced by the substrate bias voltage. The films formed at substrate bias voltage of -80 V exhibited elongated grains spread throughout the film surface. From the AFM analysis, the grain size of the films increased from 60 to 110 nm with the increase of substrate bias voltage from 0 to -80 V and at higher substrate bias voltage of -120 V it decreased to 80 nm.

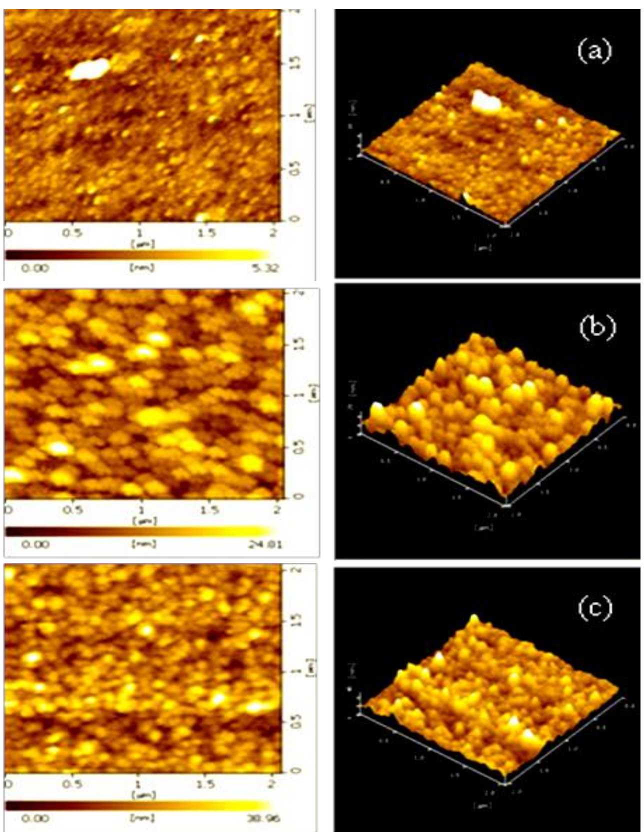

Fig. 3. Two and three dimensional AFM micrographs: (a) V_b= 0 V, (b) -80 V and (c) -120 V.

Electrical resistivity of the MZO films was measured at room temperature using four point probe method where the electric current (I) was passed in two probes and the developed voltage (V) measured in other two probes. The resistivity (ρ) of the films was calculated by using the relation,

$$\rho = (\pi/\ln 2)(V/I)t \qquad (2)$$

where, t is the thickness of the film. **Fig. 4** shows the variation in the electrical resistivity of the MZO film with substrate bias voltage. The electrical resistivity of the films formed on unbiased substrates was 8.5×10^{-1} Ωcm and it decreased to 1.2×10^{-2} Ωcm with increase of substrate bias voltage to -80 V. The decrease of resistivity with increase of substrate bias voltage was due to improvement in the crystallinity of the films. The films formed at higher substrate bias voltage of -120 V showed the electrical resistivity of 3.8×10^{-2} Ωcm. The increase of resistivity of the films formed at higher bias voltage was due to reduction in the grain size where the grain boundary scattering of charge carrier takes place hence of high resistivity. Kuo et al. [**20**] reported the electrical resistivity of 3.1×10^{-3} Ωcm in 3 wt. % Mo doped ZnO films formed by dual ion beam sputtering.

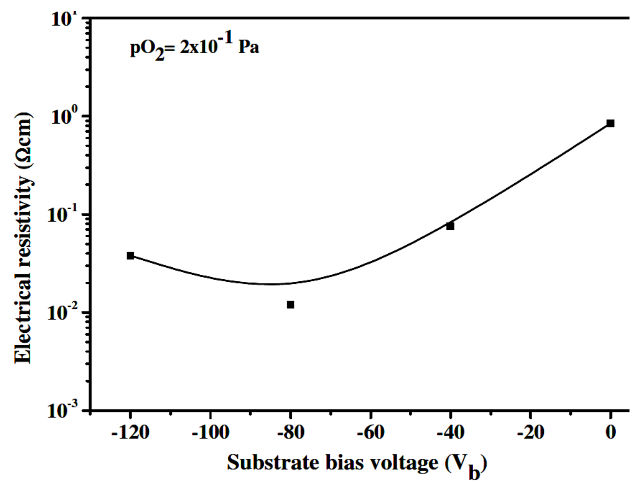

Fig. 4. Electrical resistivity of MZO films formed at different substrate bias voltages.

Fig. 5 shows optical transmittance spectra of MZO films formed at various substrate bias voltages. Optical properties of MZO films were highly influenced by the substrate bias voltage. The optical transmittance of the films in the visible region was in the range 75 - 85%.

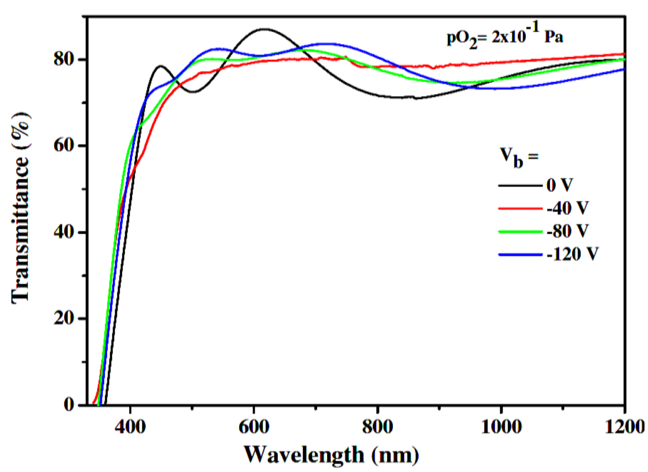

Fig. 5. Optical transmittance spectra of MZO films formed at different substrate bias voltages.

The optical absorption edge shifted towards lower wavelength side with the increase of substrate bias voltage up to -80 V there after it moved towards higher wavelength side at higher substrate bias voltage of -120 V. Wu et al. [**26**] noticed that the optical transmittance decreased from 91 to 85% with increase of Mo content from 0 to 3 wt. % in ZnO films. It is to be mentioned that the Mo-ZnO films formed by spray pyrolysis was about 60–65 % [**21**].The optical absorption coefficient (α) was determined from the transmittance (T) data using the relation,

$$\alpha = -(1/t)\ln T \quad (3)$$

The optical transitions between the valance and conduction bands of a material can be understood by studying the dependence of α on the incident photon energy (hν). For direct transition, the absorption coefficient obeys the relation,

$$\alpha h\nu = A\,(h\nu - Eg)1/2 \quad (4)$$

where, A is a constant that is edge width parameter and Eg the optical band gap. The optical band gap of the film was determined from Tauc's plots [**27**] that is the extrapolation of the linear portion of the $(\alpha h\nu)^2$ versus photon energy (hν) to α = 0. **Fig. 6** shows the plots of $(\alpha h\nu)^2$ versus photon energy of MZO films formed at different substrate bias voltages. Optical band gap of the MZO films increased from 3.18 to 3.29 eV with increase of substrate bias voltage from 0 to -80 V.

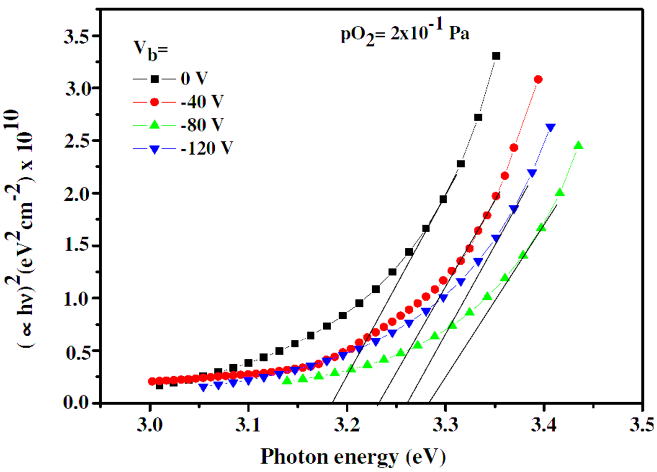

Fig. 6. Plots of $(\alpha h\nu)^2$ versus photon energy of MZO films formed at different substrate bias voltages.

The films formed at higher substrate bias voltage of -120 V showed the optical band gap of 3.27 eV. The optical band gap of 3.27 eV was also reported by Lin et al. [**28**] in pulsed DC magnetron sputtered and 3.33 eV in RF magnetron sputtered MZO films formed with molybdenum content of 2 wt. % [**26**]. The electrical resistivity and optical properties of MZO films formed by various deposition methods by different researchers are given in **Table 2.** Refractive index (n) of the films was determined from the optical transmittance interference data using the Swanepoel's envelope method [**29**].

The optical transmittance Maxima (TM) and Minima (Tm) at various wavelengths were taken from the envelope method used to determine the refractive index of the films.

The refractive index of the films was calculated using the relation,

$$n(\lambda)=[N+(N^2-n_o 2n_1 2)^{1/2}]^{1/2} \quad (5)$$

and $$N = (2n_o n_1)[(T_M-T_m)/(T_M T_m)] + [(n_o^2 + n_1^2)/2]$$

where n_o and n_1 are the refractive indices of the air and substrate respectively. Variation of refractive index with wavelength of the MZO films formed at different bias voltages are shown in **Fig. 7**. The refractive index of the films decreased with increase of wavelength from 500 to 1200 nm and remains almost constant at higher wavelengths. The refractive index of MZO films (at 500 nm) increased from 1.82 to 1.85 with increase of bias voltage from 0 to -120 V respectively.

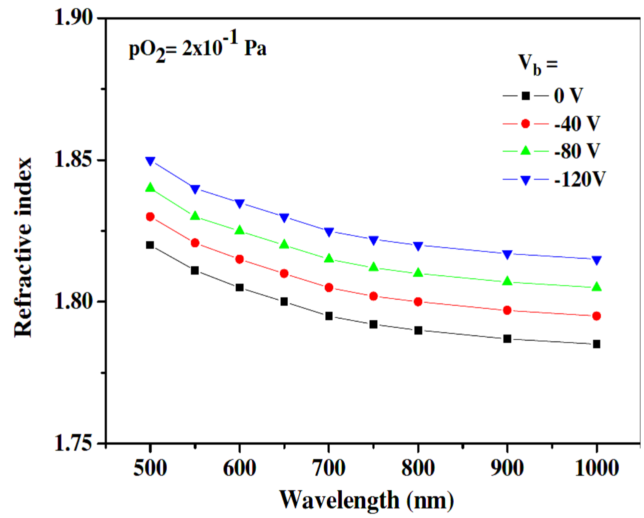

Fig. 7. Refractive index of MZO films formed at different substrate bias voltages.

The refractive index of the films is mainly influenced by the competition between the substrate and the residual molecules and the deposited film. Increase of bias voltage, plasma energy increased which enhance the diffusion ability of reactive gas molecules to form the dense films hence of increase in the refractive index [**30**]. It is to be noted that the refractive index of ZnO films formed by RF magnetron sputtering was 1.91 [**31**]. Wu et al. [**32**] achieved refractive index of 1.85 in MZO films (Mo = 3 wt. %) by DC magnetron sputtering.

Figure of merit is a quantity which gives the information about the quality of the transparent conducting oxide films. Figure of merit of MZO films was determined from the electrical resistivity and optical transmittance data. Figure of merit (φ) of the films was calculated from the relation [**33**],

$$\varphi=-1/\rho\ln T \quad (6)$$

where, ρ is the electrical resistivity of the film, T is the optical transmittance. **Fig. 8** shows the variation of the figure of merit with the substrate bias voltage. Figure of merit of the films formed unbiased substrate was 0.27 Ω-1cm^{-1}. As the substrate bias voltage increased to -80 V it increased to 19 $\Omega^{-1}cm^{-1}$.

Table 2. Summary of electrical resistivity and optical properties of MZO films

S. No	Deposition method	Molybdenum doping	Electrical resistivity (Ωcm)	Transmittance (%)	Optical band gap (eV)	Reference
1	Spray pyrolysis	2 at. %	$7x10^{-2}$	70	3.25	21
2	Ion beam sputtering	3 wt. %	$5x10^{-4}$	80	3.38	20
3	Co- sputtering	1.9 wt.%	$3.2x10^{-4}$	87	--	19
4	DC magnetron sputtering	3 wt. %	$8x10^{-4}$	85	3.80	16
5	RF magnetron sputtering	2 at. %	$9.6x10^{-4}$	85	3.35	15
6	RF magnetron sputtering	2.7 at. % V_b= -80V	$1.2x10^{-2}$	79	3.29	Present work

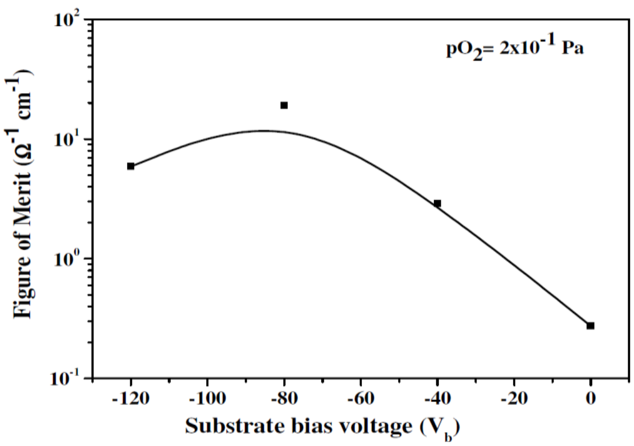

Fig. 8. Figure of merit of MZO films formed at different substrate bias voltages

Further increase of bias voltage to -120 V the figure of merit decreased to 5.9 $\Omega^{-1}cm^{-1}$. It indicated that the increase in the figure of merit was due to decrease of electrical resistivity because of better crystallinity of the films.

Conclusion

RF reactive magnetron sputtering technique was employed for deposition of molybdenum (2.7 at. %) doped zinc oxide (MZO) thin films on glass substrates. The variation of deposition rate with substrate bias voltage was due to attracting positively charged molecules and clusters in the plasma and attached on the substrate. The MZO films formed on unbiased substrates were of X-ray amorphous. Films formed at substrate bias voltage of -40 V were nanocrystalline and crystallinity improved with increase of substrate bias voltage to -80 V. The crystallite size of the films increased from 5.2 to 9.8 nm with increase of substrate bias voltage from -40 to -80 V. Atomic force microscopic studies indicated that the grain size of the films increased from 60 to 110 nm with increase of substrate bias voltage from 40 to -80 V, respectively. The electrical resistivity decreased with increase of bias voltage due to enhancement in the crystallinity of the films. The optical band gap of the films increased with increase of substrate bias voltage. In conclusion, the MZO films formed at substrate bias voltage of -80 V were of nanocrystalline with crystallite size of 9.8 nm, electrical resistivity of $1.2x10^{-2}$ Ωcm, transmittance of 79% and band gap of 3.29 eV and figure of merit of 19 $\Omega^{-1}cm^{-1}$.

Reference

1. Lupan, O.; Ghimpu, L.; Reimer, T.; Hoppe, M.; Gedamu, D.; Hammerich, D.; Chemnitz, S.; Cretu, V.; Tiginyanu, I.; Adelung., R. *J. Nanoelectron. Optoelectron*. **2014**, *9*, 257.
   DOI: 10.1166/jno.2014.1579
2. Vinod Kumar; Swart, H.C.; Som, S.; Vijay Kumar; Yousif, A.; Anurag Pandey; Shaat, S.K.K.; Ntwaeborwa, O.M. *Laser Phys.* **2014**, *24*, 105704.
   DOI: 10.1088/1054-660X/24/10/105704
3. Berrin Ikier, Sumer Peker. *Adv. Mater. Lett.* **2015**, *5*, 325.
   DOI: 10.5185/amlett.2014.amwc.10230
4. Vinod Kumar; Vijay Kumar; Som, S.; Purohit, L.P.; Nitwaeborwa, O.M.; Swart, H.C. *J. Alloys. Compounds*. **2014**, *594*, 32.
   DOI: 10.1016/j.jallcom.2014.01.110
5. Pattini, F.; Annoni, F.; Bissoli, F.; Bronzoni, M.; Garcia, J.P.; Gilioli, E.; Rampino, S. *Thin Solid Films*. **2015**, *582*, 317.
   DOI: 10.1016/j.tsf.2014.11.071
6. Liu, Y.; Lian, J. *Appl. Surf. Sci.* **2007**, *253*, 3727.
   DOI: 10.1016/j.apsusc.2006.08.012
7. Hsiao, W.T.; Tseng, S.F.; Chung, C.K.; Chiang, D.; Huang, K.C.; Lin, K.M.; Li, L.Y.; Chen, M.F. *Opt. Laser Technol.* **2015**, *68*, 41.
   DOI: 10.1016/j.optlastec.2014.11.009
8. Gurpreet Kaur; Anirbon Mitra; Yadav, K.L. *Adv. Mater. Lett.* **2015**, *6*, 73.
   DOI: 10.5185/amlett.2015.5606
9. Park, S.M.; Ikegami, T.; Ebihara, K. *Thin Solid Films*. **2006**, *513*, 90.
   DOI: 10.1016/j.tsf.2006.01.051
10. Pugalenthi, A.S.; Balasundara Prabhu, R.; Gunasekharan, V.; Muthukumarasamy, N.; Prasanna, S.; Jayakumar, S. *Mater. Sci. Semicond. Process.* **2015**, *29*, 176.
    DOI: 10.1016/massp.2014.02.014
11. Zhang, H.; Wang, R.I.; Yen, W.T.; Ha, C.T.; Peng, C. *Thin Solid Films* **2010**, *518*, 4928.
    DOI: 10.1016/j.tsf.2010.03.007
12. Oztas, M.; Bedir, M. *Thin Solid Films* **2008**, *516*, 1703.
    DOI: 10.1016/jtsf.2007.05.018
13. Yu, S.; Zhang, W.; Li, L.; Dong, H.; Xu, D.; Yin, Y.; Jin, Y. *Appl. Surf. Sci.* **2014**, *298*, 44.
    DOI: 10.1016/j.apsusc.2014.01.037
14. Larbi, T.; Ouni, B.; Boukachem, A.; Boubaker, K.; Amlouk, M. *Mater. Sci. Semicond. Process.* ***2014***, *22*, 50.
    DOI: 10.1016/j.mssp.2014.01.042
15. Wu, M.; Yu, S.; Chen, G.; He, L.; Yang, L.; Zhang, W. *Appl. Surf. Sci.* **2015**, *324*, 791.
    DOI: 10.1016/j.apsusc.2014.11.039
16. Lin, Y.C.; Wang, B.L.; Yen, W.T.; Shen, C.H. *Thin Solid Films*. **2011**, *519*, 5571.
    DOI: 10.1016/j.tsf.2011.03.014
17. Shi. Shiwei.; He Gang; Zhang Miao; Song Xueping; Li Junlei; Wang Xiao; Cul Jingbiao; Chen Xiaoshuang; Sun Zhaoqi. *Sci. Adv. Mater*. **2012**, *4*, 193.
    DOI: 10.1166/sam.2012.1272
18. Soumahoro, I.; Colis, S.; Schmerber, G.; Leuray, C.; Barre, S.; Ulhaq-Bouillet, C.; Muller, D.; Abd-lefdil, M.; Hassanian, N.; Petersen, J.; Berrada, A; Slaoui, A.; Dinia, A. *Thin Solid Films* **2014**, *566*, 61.
    DOI: 10.1016/j/tsf.2014.07.017
19. Hsu, C.M.; Lin, H.B.; Wu, W.T. *Thin Solid Films* **2009**, *517*, 3717.

DOI: 10.1016/j.tsf.2008.12.038

20. Kuo, C.C.; Liu, C.C.; He, S.C.; Chang, J.T.; He, J.L. *Vacuum* **2011**, *85*, 961.
DOI: 10.1016/j.vacuum.2011.01.018
21. Swapna, R.; Santhosh Kumar, M.C. *J. Phys. Chem. Solids.* **2013,** *74*, 418.
DOI: 10.1016/j.jpcs.2012.11.003
22. Yang, Z.W.; Han, S.H.; Yang, T.L.; Ye, L.; Zhang, D.H.; Ma, H.L.; Chang, C.H. *Thin Solid Films.* **2000**, *366*, 4.
DOI: 10.1016/S0040-6090(00)00919-6
23. Warcholinski, B.; Gilewicz, A.; Ratajski, J.; Kuklinski, Z.; Rochowicz, J. *Vacuum.* **2012**, *86*, 1235.
DOI: 10.1016/j.vacuum.2011.04.023
24. Huang, A.P.; Xu, S.L.; Zhu, M.K.; Wang, B.; Kim, H. *Appl. Phys. Lett.* **2003**, *83*, 3278.
DOI: 10.1016/j.mseb.2005.04.002
25. Subba Reddy, R.; Sivasankar Reddy, A.; Uthanna, S. *J. Optoelectron. Adv. Mater.* **2012**, *14*, 287.
DOI: 10.1016/j.optlastec.2009.09.004
31. Subba Reddy, R.; Sreedhar, A.; Sivasankar Reddy, A.; Uthanna, S. *Adv. Mater. Lett.* **2012**, *14, 287.*
DOI: 10.5185/amlett.2012.3329
32. Wu, C.;Shen, J.; Ma, J.; Wang, S.; Zhang, Z.; Yang, X. *Semicond.Sci. Technol.* **2009**, *24*, 125012.
DOI: 10.1088/0268-1242/24/12/125012
33. Haacke, G. *J. Appl. Phys.* ***1976***, *47*, 4086.
DOI: 10.1155/2012/286104